Turk Neurosurg, 2022

Original Investigation

DOI: 10.5137/1019-5149.JTN.35167-21.4

Received: 12.05.2021
Accepted: 06.11.2021

Published Online: 22.08.2022

The Effects of Necrostatin-1 on Cerebral Vasospasm-Induced Subarachnoid Hemorrhage

Mehmet Hakan SAHIN, Mehmet Emin AKYUZ, Hakan Hadi KADIOGLU

Ataturk University, School of Medicine, Department of Neurosurgery, Erzurum, Turkey

Corresponding author: Mehmet Hakan SAHIN ✉ mhsahin21@hotmail.com

ABSTRACT

AIM: To investigate the effects of necrostatin-1 (NEC-1) on subarachnoid hemorrhage (SAH)-induced vasospasm in a rat model.

MATERIAL and METHODS: A total of 59 male Wistar albino rats were randomly divided into six groups: control (group 1), sham (group 2), decapitation one hour after SAH (group 3), decapitation 48 hours after SAH (group 4), NEC-1 given 15 minutes before SAH and decapitation one hour after SAH (group 5), and NEC-1 given 24 hours after SAH and decapitation 48 hours after SAH (group 6). NEC-1 (1 uq) was administered intracisternally in dimethyl sulfoxide (DMSO) (2.6 uq). After decapitation, the cross-sectional areas and wall thicknesses of basilar arteries were determined histopathologically using stereological methods.

RESULTS: NEC-1 administered before SAH had a statistically significant preventive effect on vasospasm following SAH. Arterial wall thicknesses were found to be significantly increased in the SAH without NEC-1 groups but not in the control group, the sham group or the NEC-1 groups.

CONCLUSION: The results of this study show that NEC-1 can prevent vasospasm in rats and has cytoprotective effects. Further studies are needed for the clinical use of this agent.

KEYWORDS: Necrostatin-1, Stereology, Subarachnoid hemorrhage, Vasospasm

ABBREVIATIONS: ANOVA: Analysis of variance, **DAMP:** Damage-associated molecular patterns, **HSP:** Heat shock protein, **RIPK:** Receptor-interacting protein kinases, **TLR:** Toll-like receptors, **TNF:** Tumor necrotizing factor-alpha

INTRODUCTION

Cerebral vasospasm, cerebral ischemia, intracerebral hematoma, hydrocephalus are morbidity and mortality factors in SAH patients, and cerebral vasospasm is the most serious complication.

Despite clinical, laboratory and experimental studies for years, there are still unexplained issues regarding vasospasm. In some of the studies, it is seen that neuroinflammation plays a key role in vasospasm (12).

Neutrophils, which have a central role in the initiation of the inflammatory process after SAH, reach and accumulate in the damage zone. With the accumulation of neutrophils, the apoptotic and necrotic process begins. Apoptotic destruction plays a very important role in the resolution of inflammation. In contrast, in necroptosis caused by necrotic neutrophils, the inflammatory response is increasingly triggered by damage-associated molecular patterns (DAMPs) released from the necrotic cell wall (13).

Necrostatin-1 (NEC-1) is a “receptor interacting protein-1 (RIP1)” kinase inhibitor and is an effective and specific inhibitor of necroptosis. The neuroprotective effects of NEC-1 have been demonstrated in experimental animal studies of subarachnoid hemorrhage, traumatic brain injury, and intracerebral hematoma. It has not been previously shown that NEC-1 can be effective immunohistopathologically on cerebral vasospasm and reduce inflammation (23,25).

Mehmet Hakan SAHIN : 0000-0002-5309-4165 Mehmet Emin AKYUZ : 0000-0003-0626-3509 Hakan Hadi KADIOGLU : 0000-0002-7744-6241

MATERIAL and METHODS

Ethical approval for this study was obtained from Atatürk University Animal Experiments Ethics Committee (protocol no. 05.08.2016 / 130).

Experimental Animal Groups

A total of 59 male Wistar albino rats weighing 350 ± 50 g were used in this study. They were divided into six groups: groups 1 (anatomy study group [n=10]) and 2 (sham surgery group [n=10]) were control groups, groups 3 (decapitation one hour after SAH [n=10]) and 4 (decapitation 48 hours after SAH [n=9]) were SAH groups, groups 5 (NEC-1 given one hour after SAH and decapitation one hour after SAH [n=10]) and 6 (NEC-1 given in three doses after SAH [1st and 24th hours] and decapitation 48 hours after SAH [n=10]) were drug groups. Rats in both groups decapitated after 48 hours were given free access to food and kept at 22°C–24°C for the 48 hour period.

Induction of SAH and Drug Administration

NEC-1 (Sigma-Aldrich®, catalog no. N9037) was stored at –20°C by the manufacturer and prior to use. It was diluted at room temperature with dimethyl sulfoxide (DMSO) at the University of Atatürk School of Medicine, Medicine Biochemistry Laboratory.

Rats were subjected to fasting for eight hours before the procedure. Rats were anesthetized with intramuscular ketamine hydrochloride (50 mg/ kg) and xylazine (5 mg/ kg) and fixed to the table. After anesthesia, they were taken to the operation table in a prone position and the (previously shaved) area between occiput-C1 was determined. Cerebrospinal fluid (CSF) was drained by entering the cisterna magna trans-percutaneously with a sterile 26 G insulin injector. According to the needs of the groups, sterile saline (0.15 cc), nonheparinized autologous blood (0.15cc) or NEC-1 (2.6 uq) were injected in the same way to the cisterna magna (32). Autologous blood was taken by placing the rats in a supine position on the operation table and entering the left ventricle of the heart with a sterile insulin injector. A single intracisternal blood injection method was used to induce subarachnoid hemorrhage (21). Throughout the procedure, all animals breathed spontaneously. All subjects were decapitated after using the transcardial perfusion fixation technique and neuronal tissue was removed by occipitofrontal craniectomy (14).

After anesthesia, group 1 was decapitated after performing pre and post anesthesia procedures. In group 2, CSF (2 ml) was aspirated from each rat and an equal volume of saline was injected into the cisterna magna before decapitation. In groups 3 and 4, CSF (2 ml) was aspirated and an equal volume of fresh autologous blood was injected into the cisterna magna. The rats in group 3 were decapitated one hour after SAH and those in group 4, 48 hours after SAH. In group 5, NEC-1 (2.6 uq) was administered intracisternally 15 minutes after SAH was induced. They were decapitated after one hour of observation. In group 6, SAH was induced in rats and two doses of NEC-1 (2.6 uq) (one hour and 24 hours after SAH) were administered intracisternally and the rats were decapitated 48 hours after SAH.

Tissue Preparation

After anesthesia, a heartbeat was detected with the left-hand index finger for blood collection in the rats. Through the intercostal space lateral to the heartbeat point, we percutaneously entered the left ventricle of the heart and collected approximately 10 cc of blood. Sterile saline (10 cc) was administered into the ventricle. Afterwards, 10% formaldehyde (20 cc) was infused and perfusion fixation was completed. Approximately 10 minutes later, a craniectomy extending from the foramen magnum to the frontal region was performed and the brain tissue was removed and placed in formaldehyde (17).

The tissues taken from the rats were prepared in the Pathology Laboratory of the Medical Faculty of Atatürk University for histological examination. Histological examinations were carried out in Atatürk University Medical Faculty Histology and Embryology Laboratory.

The brain tissues were removed by craniectomy extending from the foramen magnum to the frontal region. Considering the anatomical course of the basilar artery of the brain tissues, sections were taken from the proximal, middle, and distal parts, with the upper border being the junction point of the mammary bodies, the lower border pons, and the bulbus. For the procedure, monitoring was performed using a tissue tracking device (Tissue-Tek VIP, SAKURA®).

Histological examination

The tissues were embedded in paraffin blocks. Sections of 0.5 micrometers (μm) thickness were taken and hematoxylin & eosin and TUNEL dyes were applied. Three sections from the proximal, middle, and distal parts of each basal artery were examined at 10x, 100x, and 200x magnifications.

Two pathologists who did not know the distribution of the groups examined the tissue samples under a light microscope (Leica) on a computer using Stereo Investigator (MBF® Bioscience) software. The program was used to measure the basilar artery lumen areas and photograph the sections. The artery lumen areas of the three different sections of the basilar artery were determined metrically along the endothelial layers by the software. The average of the three sections was recorded as the final value. The arterial wall thicknesses were determined by measuring the three different sections of the basilar artery of each route.

Statistical Analyses

The mean basilar artery lumen area of each subject and the mean basilar artery lumen areas of the groups, the basilar artery wall thickness, and the average basilar artery wall thickness of the groups were measured stereologically and the results were subjected to a one-way ANOVA (analysis of variance).

RESULTS

Macroscopic Review

Brain samples taken from groups 1 and 2 had the appearance of normal brain tissue. In the brain samples taken from groups 3 and 5, we found that the brain tissue was edematous and that red fresh blood spread visibly to the basal cisterns. It was observed that groups 4 and 6 were less edematous and dark red-black subacute bleeding was visibly spread to basal cisterns.

Histological Examination

Histological examination of the tissue from groups 1 and 2 showed similar features. Under light microscopic examination, it was seen that the intimal, medial, and adventitial layers of the artery wall had normal histological structures. The arterial lumen was open and smooth. The perivascular area and surrounding nerve tissue were histologically normal. No morphological changes were observed in the endothelial, medial, and adventitial layers in the preparations with TUNEL staining, suggesting apoptosis (Figures 1A, 1B, 2A, and 2B).

In the histological examination of the tissue from group 3, the preparations with H&E staining showed tortuosity in the endothelial layer, increased vessel wall thickness, and decreased vessel lumen areas. Cytoplasmic vacuolization and swelling were observed in the smooth muscle cells. No morphological changes were observed in the endothelial, medial, and adventitial layers in the preparations with TUNEL staining, suggesting apoptosis (Figures 1C and 2C).

In the histological examination of the tissue from group 4, the preparations with H&E staining showed protrusion of the nuclei of the endothelial cells toward the lumen, the lamina elastica interna was curved, and there was significant contraction of the medial layer smooth muscle cells. In addition, cytoplasmic vacuolization was observed in some of the smooth muscle cells. Significant morphological changes suggestive of apoptosis were observed in preparations with TUNEL staining (Figures 1D and 2D).

In the histological examination of the tissue from group 5, the preparations with H&E staining had folds in the endothelial layer, the vessel wall thickness and vessel lumen area did not increase significantly, and cytoplasmic vacuolization was not observed morphologically in the medial layer smooth muscle cells. Morphological changes that suggest apoptosis were not observed in each of the endothelial, medial and adventitial layers in the preparations with TUNEL staining (Figures 1E and 2E)

In the histological examination of the tissue from group 6, the preparations with H&E staining, folds in the endothelial layer were observed and the vessel wall thickness and vessel lumen area were increased. Apoptosis of the endothelium, medial, and adventitial layers was observed in the preparations with TUNEL staining. The nuclei of the endothelial cells protruded toward the lumen, the lamina elastica interna was curved, and there was contraction of the medial layer smooth muscle cells. In addition, cytoplasmic vacuolization was observed in smooth muscle cells (Figures 1F and 2F).

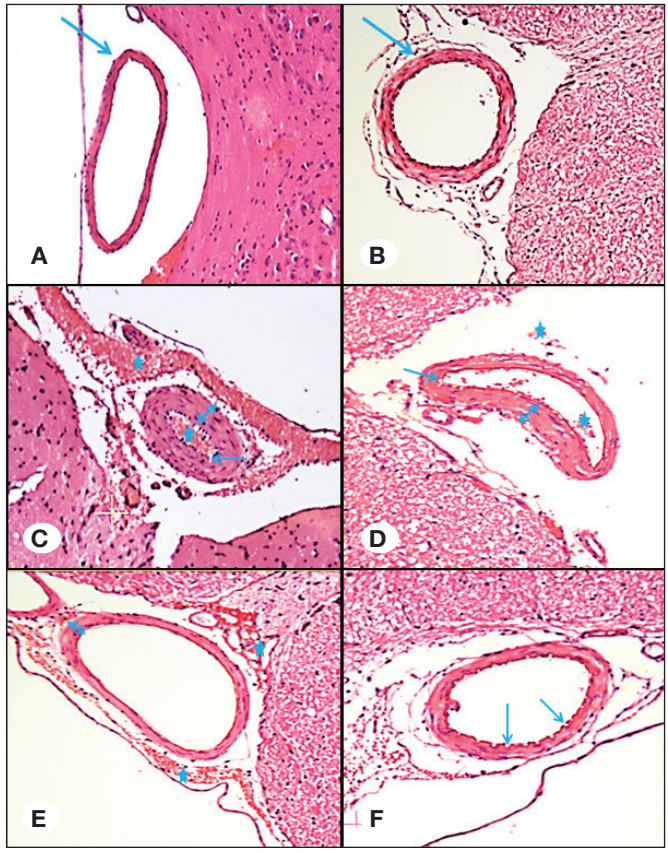

Figure 1: A) Section of the basilar artery of a control group subject. Normal morphology (blue arrow). H&E x100. **B)** Section of the basilar artery of a sham group subject. Normal morphology (blue arrow). H&E x100. **C)** Section of the basilar artery of a subarachnoid hemorrhage group subject. Vasoconstriction in the basilar artery lumen area, thickening of the vessel wall (double-ended blue arrow), endothelial tortuosity (blue arrow), and blood components in the perivascular area (blue star) of the subarachnoid space are all apparent. H&E x100. **D)** Section of the basilar artery of a subject from the group decapitated 48 hours after subarachnoid hemorrhage was observed. Vasoconstriction in the basilar artery lumen area, thickening of the vessel wall (double-ended blue arrow), endothelium tortuosity (blue arrows), and blood elements in the perivascular area (blue stars) of the subarachnoid space are all apparent. H&E x100. **E)** Section of the basilar artery of a subject from the group in which NEC-1 was given prophylactically, a basilar artery section belonging prior to the group in which SAH was formed is seen formation of the subarachnoid hemorrhage. There are blood elements in the basilar artery and in the subarachnoid space around the vessel (blue star). The vessel wall thickness and vessel lumen area does are not increase significantly increased (double -ended blue arrows). H&E, x100. **F)** Section of the basilar artery of a subject from the group in which NEC-1 was given 24 hours after SAH and subjects were decapitated 48 hours after subarachnoid hemorrhage. The basilar artery wall thickness and vessel lumen area are close to those in the control group. Unlike the control group, wrinkling of the endothelial line is prominent (blue arrows). H&E x100.

Stereological Examination and Statistical Evaluation

The mean luminal area of the Basilar Artery was detected as 612 μm² in group 1, 583 μm² in group 2, 296 μm² in group 3, 558 μm² in group 4, 559 μm² in group 5, and 527 μm² in group 6. The mean vascular lumen areas and the relationships between the groups were examined (Table I and Figure 3).

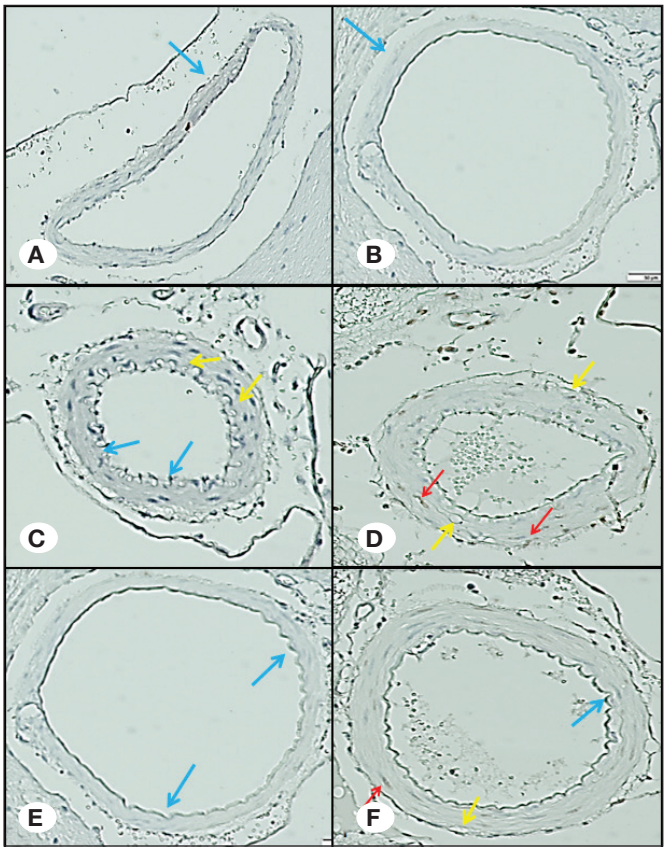

Figure 2: A) Section of the basilar artery of a sham group subject. No apoptotic/necroptotic cell death (blue arrow) occurred. TUNEL x200. **B)** A basilar artery section belonging to the sham group is seen. Basilar artery view without apoptotic / necroptotic cell death (blue arrow), TUNEL, x200. **C)** Section of the basilar artery of a subarachnoid hemorrhage group subject. Prominent wrinkling is apparent in the endothelial line (blue arrows). There is cytoplasmic vacuolization (yellow arrow) and no apoptotic/ necroptotic cell death. TUNEL x200. **D)** Section of the basilar artery of a subject from the group decapitated 48 hours after subarachnoid hemorrhage was observed. Cytoplasmic vacuolization in the vessel wall (yellow arrows) and apoptotic cell death in each of the endothelial, medial, and adventitial layers (red arrows) can be seen. TUNEL x200. **E)** Section of the basilar artery of a subject from the group in which NEC-1 was given prophylactically prior to the formation of the subarachnoid hemorrhage. Wrinkling of the endothelial line (blue arrows) is apparent. There is no apoptotic-necroptotic cell death. TUNEL x200. **F)** Section of the basilar artery of a subject from the group in which NEC-1 was given 24 hours after SAH and subjects were decapitated 48 hours after subarachnoid hemorrhage. Cytoplasmic vacuolization (yellow arrow) and TUNEL-positive intimal, medial, and adventitial layers of the basilar artery (red arrows) are seen in the vessel wall. Wrinkling (blue arrow) is apparent in the endothelial line. TUNEL x200.

Group 1: The difference between this group and groups 5 and 6 were statistically significant.

Group 2: The difference between this group and group 3 was statistically significant.

Group 3: The difference between this group and all of the other groups was statistically significant (p<0.001).

Group 4: The difference between this group and group 3 was highly statistically significant (p<0.001).

Group 5: The difference between this group and group 3 was highly statistically significant (p<0.001).

Group 6: The difference between this group and group 3 was highly statistically significant (p<0.001). The difference between this group and group 6 was also significant (p<0.01).

The mean wall thickness of the Basilar Artery was found to be 21.1 mm in group 1, 22.4 mm in group 2, 27.8 mm in group 3, 23.8 mm in group 4, 21.6 mm in group 5, and 23.7 mm in group 6. The average vascular wall thickness differences between the groups were examined (Table II and Figure 4).

Group 1: The difference between this group and groups 3, 4, and 6 were very significant. The differences between this group and group 2 and this group and group 5 were not statistically significant.

Table I: Basilar Artery Average Lumen Areas Measured Stereologically

Groups	Basilar Artery Lumen Area (μm²)
Group 1	612.3280 ± 142.07140
Group 2	583.5290 ± 68.37807
Group 3	296.1580 ± 35.62382
Group 4	558.4230 ± 54.29899
Group 5	559.4620 ± 54.29899
Group 6	527.6440 ± 47.61757

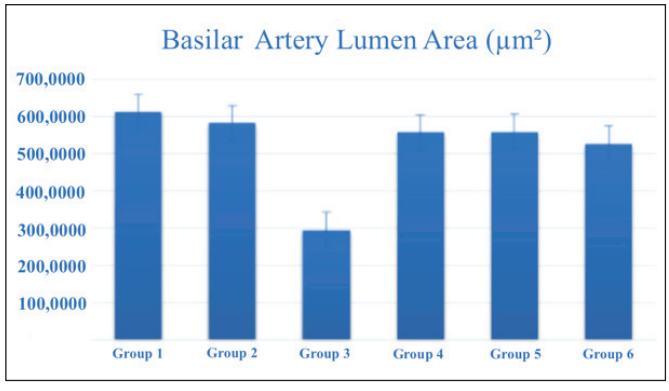

Figure 3: Statistical evaluation of basilar artery lumen areas.

Table II: Basilar Artery Average Wall Thicknesses Measured Stereologically

Groups	Basilar Artery Wall Thickness (μm)
Group 1	21.1200 ± 1.07269
Group 2	22.4300 ± 1.37925
Group 3	27.8000 ± 2.73496
Group 4	23.8500 ± 1.12571
Group 5	21.6400 ± 0.87965
Group 6	23.7500 ± 1.59878

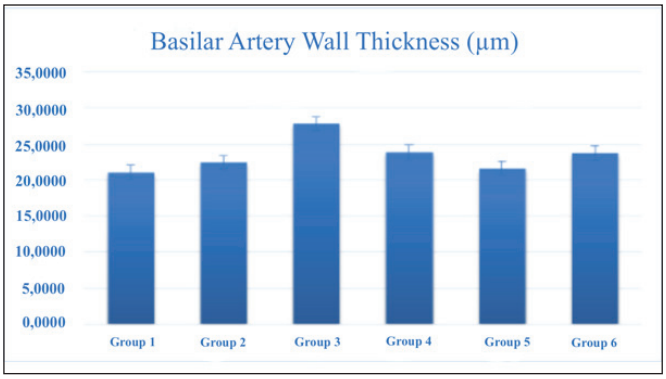

Figure 4: Statistical evaluation of basilar artery wall thickness.

Group 2: The difference between this group and group 3 was statistically significant.

Group 3: The difference between this group and groups 1, 2, and 5 were very significant ($p<0.001$). The difference between this group and groups 4 and 6 were also significant ($p<0.01$).

Group 4: The difference between this group and group 3 was very significant ($p<0.05$). The differences between this group and groups 4 and 6 were less significant. The differences between this group and the other groups were not statistically significant.

Group 5: The difference between this group and group 3 was very significant ($p<0.001$). The difference between this group and groups 4 and 6 were also significant ($p<0.01$). The differences between this group and the other groups were not statistically significant.

Group 6: The difference between this group and groups 1 and 3 were very significant ($p<0.001$). The difference between this group and group 5 was also significant ($p<0.05$). The differences between this group and the other groups were not statistically significant.

DISCUSSION

SAH is a serious cause of morbidity and mortality. Aneurysms are the most common feature of non-traumatic SAHs. Many complications affect the outcome of aneurysmal subarachnoid hemorrhages, the most serious of which is vasospasm. The pathogenesis of vasospasm is not yet fully understood. The process begins when blood that has extravasated into the subarachnoid space causes contraction of the vascular smooth muscle (12,16). In vasospasms observed after SAH, the intimal, medial, and adventitial layers of the cerebral arteries are affected and morphologically pathological changes are observed in these layers (1).

Many mechanisms are thought to be involved in the pathogenesis of cerebral vasospasm. Among these, inflammation plays a decisive role. It is thought that inflammation affecting the endothelium disrupts the blood-brain barrier, stimulating the contraction of the vascular smooth muscles and resulting in vasospasm. Supporting this theory is the finding that vasodilator agents, which are frequently used in the treatment of vasospasm, are radiologically effective. However, they do not provide the same improvements in the early and late neurological status of patients (1,27).

There are numerous mediators of the inflammation thought to cause vasospasm. Inflammatory mediators such as E-selectin, TNFa, IL-1, IL-6, and IL-8 are thought to play a role in vasospasm after SAH. These appear to increase at different rates in different studies (1,9,11).

Vasospasm develops after intracisternal administration of various pro-inflammatory agents, including talc, latex, polystyrene, dextran lipopolysaccharide, and tenascin-C. Also, the amount of blood in the subarachnoid space can affect the cytokine levels in the CSF. Inflammation contributes to both tissue damage and tissue healing by causing vasospasm after (10,11,20).

Neurological deterioration in most SAH patients is due to cerebral vasospasm, which peaks 7 to 14 days after SAH, although such deterioration but may also occur in the absence of vasospasm. Clinically, the presence of cell death, cerebral edema, and vasospasm predict a poor prognosis after SAH. A correlation has been demonstrated between hippocampal neuronal loss and increased neurofilament levels in the CSF, axonal disruption, and clinical outcomes after SAH. Blocking inflammatory pathways after SAH can both prevent blood-brain barrier disruption and increase neuronal survival (3,8). Cell death is an important biological process. Apoptosis, necrosis and necroptosis are types of cell death. Apoptosis is an anti-inflammatory process and programmed cell death. (6,21). In contrast, necrosis leads to the rapid loss of plasma membrane integrity. Early plasma membrane rupture in necrosis releases DAMP, which are powerful stimulants of inflammation (15). Pathologists have historically relied on morphology to distinguish between apoptosis and necrosis but classical markers of apoptosis are sometimes found in necrosis. Thus, morphological distinctions between apoptosis and necrosis are insufficient. Programmed necrosis, regulated necrosis or necroptosis is a type of cell death that occurs via a genetic pathway mediated by receptor-interacting protein kinases (RIPK) (18). There are overlapping signal centers on the pathways that control necroptosis and inflammation. The use of common signaling pathways establish a close link between inflammation and necroptosis (22).

Necroptosis is activated by the death receptors of the TNR superfamily: TLR3, TLR4, and interferon receptors. The signaling pathway for necroptosis is best characterized by the TNFR1 receptor. The signal formed after the ligation of TNFR1 trimmer with TNF causes conformational changes to the short-lived membrane-signal complex, complex I. A transition from complex I to complex II is triggered by activation of conserved cylindromatosis (CYLD), which has the chain structure of ubiquitin. When caspase-8 is disabled or absent, RIPK1 and RIPK3 do not disintegrate and eventually phosphorylate. This then creates a necrosome and causes cell necroptosis (24).

The combination of phosphorylated RIPK1 and RIPK3 form a RIP complex and transmit a signal by providing phosphorylation to the MLKL protein, resulting in tetramers and initiating Ca_2 + entry into the plasma membrane. This causes translocation (2). With membrane integrity disrupted, new DAMP proteins trigger more necroptosis. It is still unclear whether the molecular transition mechanism decides whether apoptosis or necroptosis will occur. Necroptosis is independent of caspase and cannot be inhibited by caspase inhibitors. Necroptosis is thought to be pro-inflammatory. Animal studies have revealed that it plays an important role in the pathogenesis of inflammatory diseases. Necroptosis has also been shown to cause the release of DAMPs, which are molecular patterns associated with damage. DAMPs in the extracellular environment trigger inflammation and this leads to a chain reaction (6,19).

Because of the role of RIPK1 and RIPK3 in necroptosis, inhibition of these enzymes is thought to be a good means of preventing necroptosis. To this end, RIP-1-specific NEC-1 was found. Necrostatins have proven very useful in animal disease models (7,26). Recent studies have shown NEC-1 to have neuroprotective properties after SAH (4,5).

In our experiment, TUNEL staining, which is an indicator of apoptosis/ necroptosis, was observed in the histopathological preparations from groups 4 and 6. When these two groups were compared, it was observed that the endothelial, medial, and adventitial layers of the NEC-1 treated group retained less TUNEL staining and fewer endothelial folds than group 4. There were no significant differences between these two groups in terms of vessel lumen area or vessel wall thickness. NEC-1 given after subarachnoid hemorrhage reduced inflammation but did not significantly reduce vasospasm. TUNEL staining in groups 3 and 5 was not informative regarding inflammation in the early period of SAH. The basilar artery lumen area and basilar artery wall thickness of all of the groups were compared and statistically significant differences were seen between group 3 and group 5 and between group 3 and group 6.

CONCLUSION

This study demonstrated that prophylactic NEC-1 reduces vasospasm in the early period after SAH. On the other hand, it was observed that NEC-1 given after SAH reduced inflammation but had no significant effect on vasospasm. Thus, it has been shown that NEC-1 may be effective on vasospasm in the early stage of SAH. Further studies are needed for the clinical use of this agent.

ACKNOWLEDGEMENTS

As the author was unable to find funding, more specific histopathological stains could not be made to show the inflammatory activity of the drug. Histopathological staining was only sufficient to show vasospasm.

I would like to thank the academicians who examined our pathology preparations and contributed to the statistical analysis. I would also like to thank the lab staff for their assistance throughout the experiment.

AUTHORSHIP CONTRIBUTION

Study conception and design: HHK

Data collection: MHS

Analysis and interpretation of results: MHS

Draft manuscript preparation: MEA

Critical revision of the article: HHK

Other (study supervision, fundings, materials, etc...): MEA

All authors (MHS, MEA, HHK) reviewed the results and approved the final version of the manuscript.

REFERENCES

1. Borel CO, McKee A, Parra A, Haglund MM, Solan A, Prabhakar V, Sheng H, Warner DS, Niklason L: Possible role for vascular cell proliferation in cerebral vasospasm after subarachnoid hemorrhage. Stroke 34:427-33, 2003
2. Cai Z, Jitkaew S, Zhao J, Chiang HC, Choksi S, Liu J, Ward Y, Wu LG, Liu ZG: Plasma membrane translocation of trimerized MLKL protein is required for TNF-induced necroptosis. Nat Cell Biol 16:55-65, 2014
3. Caner B, Hou J, Altay O, Fujii M, Zhang JH: Transition of research focus from vasospasm to early brain injury after subarachnoid hemorrhage. J Neurochem 2:12-21, 2012
4. Chen F, Su X, Lin Z, Lin Y, Yu L, Cai J, Kang D, Hu L: Necrostatin-1 attenuates early brain injury after subarachnoid hemorrhage in rats by inhibiting necroptosis. Neuropsychiatr Dis Treat 13:1771-1782, 2017
5. Chen J, Jin H, Xu H, Peng Y, Jie L, Xu D, Chen L, Li T, Fan L, He P, Ying G, Gu C, Wang C, Wang L, Chen G: The neuroprotective effects of necrostatin-1 on subarachnoid hemorrhage in rats are possibly mediated by preventing blood-brain barrier disruption and RIP3-mediated necroptosis. Cell Transplant 28:1358-1372, 2019
6. Davidovich P, Kearney CJ, Martin SJ: Inflammatory outcomes of apoptosis, necrosis and necroptosis. Biol Chem 395:1163-1171, 2014
7. Degterev A, Hitomi J, Germscheid M, Ch'en IL, Korkina O, Teng X, Abbott D, Cuny GD, Yuan C, Wagner G, Hedrick SM, Gerber SA, Lugovskoy A, Yuan J: Identification of RIP1 kinase as a specific cellular target of necrostatins. Nat Chem Biol 4:313-321, 2008
8. Donnelly DJ, Popovich PG: Inflammation and its role in neuroprotection, axonal regeneration and functional recovery after spinal cord injury. Exp Neurol 209:378-388, 2008

9. Fassbender K, Hodapp B, Rossol S, Bertsch T, Schmeck J, Schütt S, Fritzinger M, Horn P, Vajkoczy P, Kreisel S, Brunner J, Schmiedek P, Hennerici M: Inflammatory cytokines in subarachnoid haemorrhage: Association with abnormal blood flow velocities in basal cerebral arteries. J Neurol Neurosurg Psychiatry 70:534-537, 2001
10. Fujimoto M, Suzuki H, Shiba M, Shimojo N, Imanaka-Yoshida K, Yoshida T, Kanamaru K, Matsushima S, Takia W: Tenascin-C induces prolonged constriction of cerebral arteries in rats. Neurobiol Dis 55:104-109, 2013
11. Gaetani P, Tartara F, Pignatti P, Tancioni F, Baena RR, De Benedetti F: Cisternal CSF levels of cytokines after subarachnoid hemorrhage. Neurol Res 20:337-342, 1998
12. Grasso G, Alafaci C, Macdonald RL: Management of aneurysmal subarachnoid hemorrhage: State of the art and future perspectives. Surg Neurol Int 19:8:11, 2017
13. Jie H, He Y, Huang X, Zhou Q, Han Y, Li X, Bai Y, Sun E: Necrostatin-1 enhances the resolution of inflammation by specifically inducing neutrophil apoptosis. Oncotarget 12: 19367-19381, 2016
14. Kasukurthi R, Brenner MJ, Moore AM, Moradzadeh A, Ray WZ, Santosa KB, Mackinnon SE, Hunter DA: Transcardial perfusion versus immersion fixation for assessment of peripheral nerve regeneration. J Neurosci Methods 184:303-309, 2009
15. Kono H, Rock KL: How dying cells alert the immune system to danger. Nat Rev Immunol 8:279-289, 2008
16. Lucke-Wold BP, Logsdon AF, Manoranjan B, Turner RC, McConnell E, Vates GE, Huber JD, Rosen CL, Simard JM: Aneurysmal subarachnoid hemorrhage and neuroinflammation: A comprehensive review. Int J Mol Sci 17: 497, 2016
17. Marbacher S, Fandino J, Kitchen ND: Standard intracranial in vivo animal models of delayed cerebral vasospasm. Br J Neurosurg 24:415-434, 2010
18. Moriwaki K, Chan FK: RIP3: A molecular switch for necrosis and inflammation. Genes Dev 27:1640-1649, 2013
19. Pasparakis M, Vandenabeele P: Necroptosis and its role in inflammation. Nature 517: 311-320, 2015
20. Recinos PF, Pradilla G, Thai QA, Perez M, Hdeib AM, Tamargo RJ: Controlled release of lipopolysaccharide in the subarachnoid space of rabbits induces chronic vasospasm in the absence of blood. Surg Neurol 66:463-469, 2006
21. Segawa K, Kurata S, Yanagihashi Y, Brummelkamp TR, Matsuda F, Nagata S: Caspase-mediated cleavage of phospholipid flippase for apoptotic phosphatidylserine exposure. Science 344:1164-1168, 2014
22. Sosna J, Voigt S, Mathieu S, Lange A, Thon L, Davarnia P, Herdegen T, Linkermann A, Rittger A, Ka-Ming Chan F, Kabelitz D, Schütze S, Adam D: TNF-induced necroptosis and PARP-1mediated necrosis represent distinct routes to programmed necrotic cell death. Cell Mol Life Sci 71:331-348, 2014
23. Vandenabeele P, Galluzzi L, Vanden Berghe T, Kroemer G: Molecular mechanisms of necroptosis: An ordered cellular explosion. Nat Rev Mol Cell Biol 11:700-714, 2010
24. Vanlangenakker N, Bertrand MJ, Bogaert P, Vandenabeele P, Vanden Berghe T: TNF-induced necroptosis in L929 cells is tightly regulated by multiple TNFR1 complex I and II members. Cell Death Dis 2:e230, 2011
25. Wang YQ, Wang L, Zhang MY, Wang T, Bao HJ, Liu WL, Dai DK, Zhang L, Chang P, Dong WW, Chen XP, Tao LY: Necrostatin-1 suppresses autophagy and apoptosis in mice traumatic brain injury model. Neurochem Res 37:1849-1858, 2012
26. Zhou Z, Han V, Han J: New components of the necroptotic pathway. Protein Cell 3:811-817, 2012
27. Zubkov AY, Ogihara K, Bernanke DH, Parent AD, Zhang J: Apoptosis of endothelial cells in vessels affected by cerebral vasospasm. Surg Neurol 53:260-266, 2000